

¹⁵J. Hermanson, Phys. Rev. **166**, 893 (1968); Phys. Rev. Lett. **18**, 170 (1967); Y. Toyozawa, M. Inoue, T. Inui, M. Okazaki, and E. Hanamura, J. Phys. Soc. Jap. **22**, 1337 (1967); J. Phys. Soc. Jap. **22**, 1349 (1967).

¹⁶J. Kanamori, J. Appl. Phys. Suppl. **36**, 429 (1965); F. Gautier and P. Lengart, Phys. Rev. **139**, A705 (1965).

¹⁷F. Stern, Phys. Rev. **158**, 697 (1967); J. Callaway and A. J. Hughes, Phys. Rev. **156**, 860 (1967).

¹⁸W. M. Hartman (private communication); C. M. Varma, Phys. Rev. A **4**, 313 (1971).

¹⁹M. Hamermesh, *Group Theory* (Addison-Wesley, Reading, Mass., 1962), Chaps. 2-4.

²⁰L. P. Bouckaert, R. Smolouchowski, and E. Wigner, Phys. Rev. **50**, 58 (1936). See also J. Callaway, *Energy Band Theory* (Academic, New York, 1964), Chap. 1.

²¹Second of Refs. 8; and H. Callen and V. G. Baryakhtar, Phys. Rev. B **6**, 1010 (1972).

²²F. J. Blatt, Phys. Rev. **108**, 285 (1957).

²³A. M. Clogston, Phys. Rev. **136**, A1417 (1964).

²⁴J. Hubbard, Proc. R. Soc. A **281**, 401 (1964); N. F. Mott, Rep. Prog. Phys. **33**, 88 (1970).

²⁵W. Kohn and Majumdar, Phys. Rev. **138**, A1617 (1965).

²⁶For the FSA prediction see Ref. 7.

²⁷For the residual resistivity expression for an isotropic material see Ref. 1, p. 188.

²⁸B. W. Veal and J. A. Rayne, Phys. Rev. **130**, 2156 (1963); U. Mizutani, S. Noguchi, and T. B. Massalski, Phys. Rev. B **5**, 2057 (1972).

²⁹J. A. Blackman, D. M. Esterling, and N. F. Berk, Phys. Lett. A **35**, 205 (1971); Phys. Rev. B **4**, 2412 (1971).

Temperature Dependence of the Electron Relaxation Time in Thallium Measured by the Radio-Frequency Size Effect*

James E. Bradfield[†] and Julian B. Coon

Department of Physics, University of Houston, Houston, Texas 77004

(Received 8 December 1972)

The temperature dependence of the electron scattering time τ averaged over an orbit has been investigated in thallium using the radio-frequency size effect. It was found that τ fit an expression of the form $1/\tau = a + bT^n$. For closed orbits the temperature exponent varied from $n = 3$ at low magnetic fields to $n = 5$ at high values of the magnetic field. A scattering-effectiveness criterion was introduced and was used to predict a magnetic field dependence for n in agreement with experiment. The value of the deformation potential averaged over an orbit was obtained for orbits with $n = 3$.

I. INTRODUCTION

The temperature dependence of the relaxation time for electrons in metals has been the subject of several recent investigations. Various techniques including radio-frequency size effects (RFSE),¹⁻⁷ ultrasonic attenuation,⁸⁻¹⁵ cyclotron resonance,¹⁶ bulk-resistivity measurements,¹⁷⁻²⁰ and magnetic-surface-state resonance²¹⁻²⁷ have been employed by experimenters, yielding a variety of results. Generally, however, it is found that the relaxation time τ varies according to $1/\tau = a + bT^n$ for temperatures in the range 0 to 10°K, where n assumes values between $n = 2$ and $n = 7$.

The experimental results may be understood by assuming that an electron on a resonant orbit undergoes a scattering event in an average time τ which removes the electron from the resonant orbit. If one also assumes that collisions with impurities and with the lattice (in the form of electron-phonon interactions) contribute to the total scattering rate independently, the expression for τ may be written as $1/\tau = 1/\tau_i + 1/\tau_p$, where $1/\tau_i$ is the average scattering frequency due to impurities and $1/\tau_p$ is the electron-phonon scattering frequency. τ_i is temperature independent over the

range of temperatures investigated.

A model for electron-phonon scattering in which it is assumed that every electron-phonon collision is effective in removing the electron from the resonant orbit results in an expression of the form

$$1/\tau_p = \frac{|C_0|^2}{8\pi^2 N M C_s} \int [n_{\vec{q}}(1 - f_{\vec{k} + \vec{q}})\delta(E_{\vec{k} + \vec{q}} - h\omega_{\vec{q}} - E_{\vec{k}}) + (n_{\vec{q}} + 1)(1 - f_{\vec{k} - \vec{q}})\delta(E_{\vec{k} - \vec{q}} + h\omega_{\vec{q}} - E_{\vec{k}})] q d^3q,$$

corresponding to processes of emission and absorption of a phonon of wave vector \vec{q} . (M is the ion mass, C_s is the velocity of sound, and C_0 is the average deformation potential.) In the Debye approximation and at low temperatures the integral may be evaluated and one finds $1/\tau_p = \Gamma T^3$ where

$$\Gamma = 2.4 \times 10^7 (|C_0|^2/k_D) (m_c/m)$$

for thallium where $|C_0|$ is measured in eV and k_D in units of 10^8 cm^{-1} . Thus a temperature dependence for $1/\tau$ of the form $1/\tau = a + \Gamma T^3$ is predicted. If $n = 3$ experimentally, as occurs for many orbits observed in this experiment and others, a value for the average value of the deformation potential over the orbit can be determined.

In this experiment, as well as in the work of

other investigators, values of the temperature exponent $n > 3$ have been observed, the most frequently observed result being $n = 5$. Ziman²⁸ explains the $n = 5$ result for bulk-resistivity measurements by noting that when a direct current is measured, it is the change in the component of the electron velocity parallel to the static electric field which is of importance. Thus a factor proportional to $(\vec{v}_E - \vec{v}_E) \cdot \vec{E}$ introduces a factor of $(1 - \cos\theta)$ as an effectiveness weighting factor into the integrals for $1/\tau$. Since for electron-phonon scattering $q \ll k_F$, then $\theta \approx q/k_F$. This results in an additional term proportional to q^2 in the integral, giving rise to the $n = 5$ exponent. Myers *et al.*⁶ use similar arguments based on the fact that as q becomes very small, multiple-scattering events become necessary in order to render an electron ineffective, again resulting in a $n = 5$ exponent. The $n = 5$ case, as well as the general case $n > 3$ is discussed further in Sec. III of this paper.

In the parallel-field RFSE,²⁹ an rf electric field is applied to the major surfaces of a thin metallic sample. In the antisymmetric excitation geometry, as used in this experiment, the rf field is in opposite directions at the major sample surfaces. Under the conditions $l \cdot d \gg \delta$, spatial resonances in the RFSE occur at magnetic fields such that $B = c\hbar k_D / ed$, where l is the electron mean free path (emfp), d is the sample thickness, δ is the rf skin depth, and k_D the orbit caliper dimension. The amplitude A of the RFSE line is proportional to the number of electrons passing through both skin-depth regions without being scattered from the resonant trajectory. Thus if L is the length of the trajectory followed by the electron in proceeding from one sample surface to the other, then

$$A \propto \frac{e^{-L/2l}}{1 - e^{-L/2l}} = \frac{e^{-\pi/\omega_c\tau}}{1 - e^{-\pi/\omega_c\tau}} \quad (1)$$

allowing for multiple passes through the skin depth before scattering. Measurement of the temperature dependence of the RFSE signal amplitude, therefore, allows the temperature dependence of τ to be determined.

II. EXPERIMENTAL

The samples used in this research were obtained from a refined 99.9999%-pure bar of thallium purchased from Cominco American Incorporated. A 2-in. long section was spark cut from the original bar and subjected to the strain-anneal technique of crystal growth. Several large crystals were produced, and the samples used in this research were cut from one of these crystals. The crystal was oriented using Laue back-reflection x-ray photographs. Rectangular samples approximately $6 \times 9 \times 2$ mm were cut from the oriented sample. Although sample orientation within 1° of

a crystalline axis was considered adequate, the faces of the sample had to be parallel to considerably better than 1° to ensure the desired 2% uniformity in the sample thickness. To produce adequate parallelness, a block of stainless steel was first spark planed to ensure that the mounting surface was parallel to the planing wheel. The sample was then mounted on the stainless steel and spark machined. Since the orientation of the planing wheel was found to change slightly over long periods of planing, the sample was removed before the final few hundredths of a mm were taken off, and the stainless steel was replaned. The damage from the spark planing was removed by applying very dilute nitric acid with a Q-tip and rinsing immediately in water. The orientation was rechecked by Laue back reflection and found to be within 1° of the desired crystal axis. The samples were stored in glycerin between experimental runs to prevent oxidation.

A micrometer gauge having a 0.0001-in. vernier was used to measure the sample thickness at each edge, each corner, and in the middle for a total of nine measurements. The thickness of the [0001] sample was 0.1655 ± 0.0038 mm. The thickness of the [0001] sample could be also determined from the period of the open orbit along AL . The Brillouin-zone dimension in the AL direction calculated from the lattice constants of Barrett³⁰ has the value $k_{BZ} = 2.1103 \pm 0.0011 \text{ \AA}^{-1}$. The open-orbit electrons produce periodic resonances that damp slowly and dominate the high-field data. The period ΔB of the resonance can be used to calculate the sample thickness d from $\hbar k_{BZ} = (e/c)d(\Delta B)$. In determining the period it is necessary to extrapolate the fiducials to the zero-skin-depth limit before measuring B as discussed in Sec. III. The result is $d = 0.1622 \pm 0.0016$ mm for the [0001] sample, which was the thickness used in the data reduction.

For another phase of this research it was necessary to design a sample holder which would allow the plane of the sample to be tilted at any angle up to 20° with respect to the magnetic field for any orientation of the magnetic field. This capability allowed the sample surfaces to be aligned parallel to the magnetic field to within 0.2° . Tilt studies were performed and were invaluable aids in orbit identification and assignment. A block diagram of the apparatus is shown in Fig. 1. An rf coil was placed around the sample and formed the inductive part of the LC tank circuit of the marginal oscillator similar to that of Shih-Yu Feng.³¹ Using a ten-turn potentiometer for the bias resistor allowed the sensitivity to be reset precisely enough so that amplitudes could be reproduced to about 2%. The detector output of the oscillator was fed into a PAR model HR-8 lock-in amplifier which also provided the sinusoidal reference used to

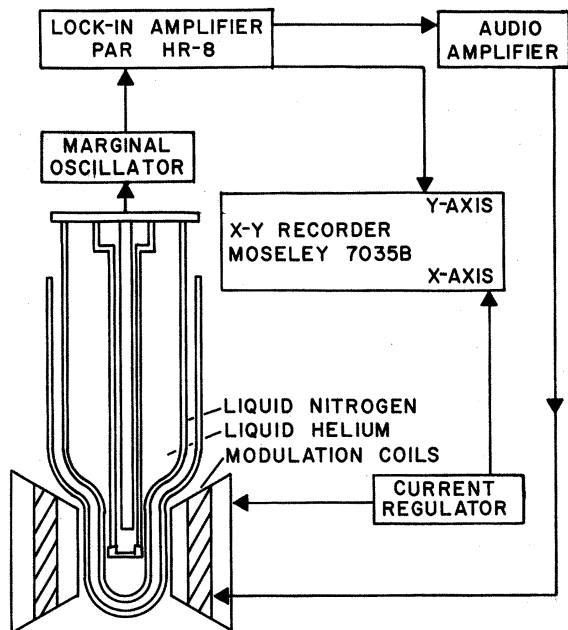


FIG. 1. A block diagram of the experimental apparatus.

drive the modulating magnetic field for phase-sensitive detection. The output of the lock-in amplifier was displayed on the y axis of an xy recorder. The x axis signal was proportional to the current through the magnet, and the magnetic field was calibrated using NMR. The resulting display was proportional to $(\partial R/\partial B)$ versus B (Figs. 2 and 3) where R is the real part of the surface impedance of the sample. At low temperatures the 2% variation in oscillator sensitivity dominated the uncertainty in the resonance amplitude. At high temperatures the amplitude is small, and the uncertainty in A is dominated by the signal-to-noise ratio. A basis for judging the over-all sensitivity of the electronics is to note the highest temperature at which resonances are still visible, and compare the temperature with that of other investigators using the RFSE in the same metal. Gage and Goodrich,³² using second-harmonic detection to plot $(\partial^2 R)/(\partial B^2)$ versus B , observed no lines above 2.2 °K. Takle and Stanford³³ observed lines up to 3.3 °K using FM detection to plot $(\partial \chi)/(\partial B)$ versus B , where χ is the imaginary part of the surface impedance. This work produced lines at temperatures as high as 3.7–3.9 °K. The temperature interval investigated in this research was 1.2 to 4.17 °K.

III. DATA ANALYSIS AND RESULTS

A. Frequency Studies and Caliper Assignment

Although the RFSE has found wide acceptance as the best experimental technique for direct mea-

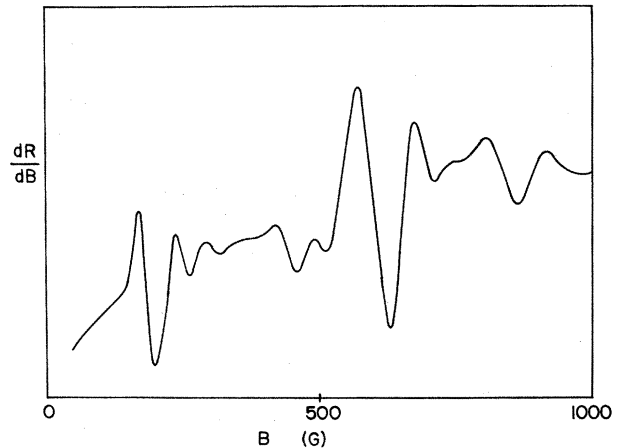


FIG. 2. A recorder tracing of dR/dB vs the magnetic field between 0 and 1 kG. The magnetic field is oriented along the $[11\bar{2}0]$ axis.

surement of Fermi surface calipers, no complete theoretical treatment exists to date which predicts the observed line shape well enough to allow the caliper field point to be determined. As a result, several empirical methods have been devised to determine the resonance field assigned to a RFSE line. Two of the more successful techniques have been discussed in detail by Jones *et al.*³⁴ and by Gage and Goodrich³² and will not be reviewed in this paper. A third technique, exploited by Cleveland and Stanford³⁵ and by Krylov³⁶ relies on the fact that the RFSE linewidth is proportional to the skin depth δ . In the anomalous skin effect region δ varies as $\omega^{-1/3}$ where ω is the frequency of the rf field. Thus if B_n is a value of the magnetic field associated with an observable feature of a RFSE

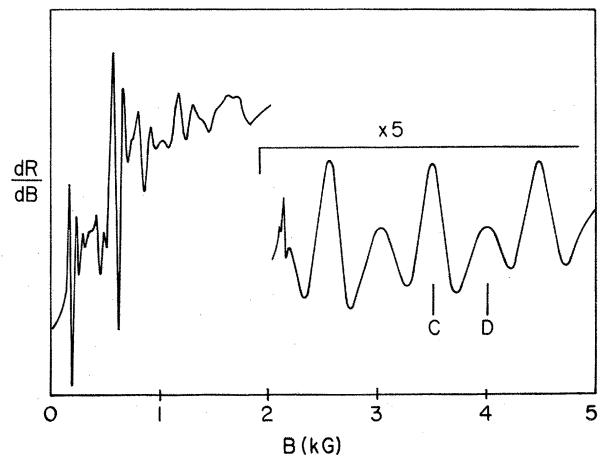


FIG. 3. A recorder tracing of dR/dB vs the magnetic field between 0 and 5 kG. The high-field oscillations are due to the AL open orbit electrons.

line arising from an orbit with a caliper k_D , one expects a relation of the form $B_n = B_0 + a\omega^{-1/3}$ to describe the frequency dependence of B_n . (B_0 is the true resonance field.) By plotting B_n versus $\omega^{-1/3}$ and extrapolating to infinite frequency, the true resonance field for the k_D may be determined.

In this research, the RFSE signal amplitude proportional to $\partial R/\partial B$ was recorded as a function of magnetic field for several frequencies. Fiducials corresponding to points of steepest slope and extrema of the signal amplitude were plotted versus $\omega^{-1/3}$. In all cases studied it was found that B_n varied as expected. Further, it was found that in most cases two or more extrapolated values of B_n coincided within 2% for a particular RFSE line as shown in Fig. 4. As is also illustrated in Fig. 4, some RFSE lines due to different orbits overlap as a function of magnetic field. By using the frequency-extrapolation technique, it was found that signals with complicated line shapes due to overlap could be resolved into their separate components, allowing an unambiguous caliper determination. All orbits identified in this research are assigned in this manner. The reported resonant fields are the extrapolated values corresponding to the intersection of two or more frequency extrapolations.

While it was not the major emphasis of this research to caliper the Fermi surface of thallium,

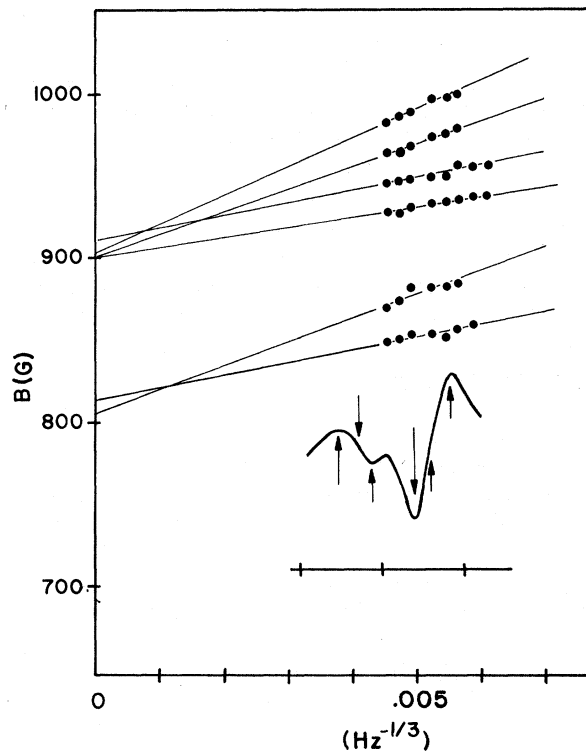


FIG. 4. A plot of B_n vs $\omega^{-1/3}$ indicating convergence of resonant field points.

it was necessary to make RFSE line and caliper assignments as part of the relaxation-time study. (The Brillouin zone of thallium is shown in Fig. 5.) Sufficient data were taken about the crystal symmetry directions to determine the angular dependence of the caliper as well as the numerical value. These results along with the results of the tilt study were used in making caliper assignments. The results for the [0001] sample are reported in Table I and are in general agreement with those of previous workers. However, the angular and tilt dependence of the i series observed in this research suggested that a caliper of 0.49 be assigned to the orbit shown in Fig. 6, in apparent disagreement with Gage and Goodrich. The f series, which produced a signal which overlapped the i series resonance and was resolved using the frequency extrapolation technique, would be assigned to an intermediate orbit such as that shown in Fig. 6.

B. Temperature Dependence

The temperature dependence of the electron scattering time, τ , was determined from the experimental data using Eq. (1) and $1/\tau = a + bT^n$. In all cases it was observed that the temperature dependence of the RFSE signal amplitude obeyed a relation of the form $A \propto e^{-\pi/\omega_c\tau}$ equally as well as Eq. (1), indicating that $\omega_c\tau \lesssim 1$, i.e., the effect of multiple passage through the skin depth could be neglected. The temperature exponent n was obtained by plotting the natural logarithm of the signal amplitude versus T^n for each resonance and selecting that value of n which resulted in the best straight-line fit. A sample set of curves is shown in Fig. 7.

The temperature dependence of τ averaged over an electron orbit was investigated for several orbits and the results are summarized in Table I. Below 800 G all the orbits studied showed the expected $1/\tau_p = \Gamma T^3$ dependence characteristic of a single electron-phonon scattering event being sufficient to render the electron on the orbit ineffective. The constant Γ can be evaluated by determining the slope of the $\ln A$ versus T^3 plot for those orbits with $n=3$. In addition, it is necessary to know ω_c at the resonant field. This quantity was estimated using the relation $\omega_c = \hbar k_D / m_c d$ at the resonance field, which is exact for a spherical Fermi surface. Thus a value of the average scalar deformation potential, $|C_0|$, over the orbit can be determined according to

$$|\text{slope}| = \frac{2\pi m_c d \Gamma}{\hbar k_D} = 5.28 \times 10^3 \frac{|C_0|^2}{k_D^2} \left(\frac{m_c}{m}\right)^2, \quad (2)$$

where $|C_0|$ is in eV and k_D is in units of 10^8 cm^{-1} . The results of the calculations are shown in Table I. Wherever possible, the experimentally determined values of m_c and k_D were used for each

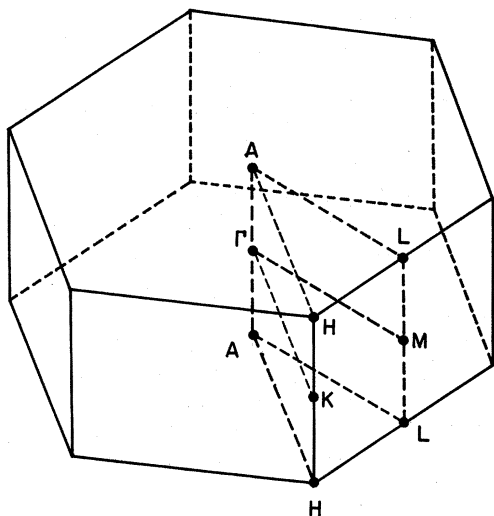


FIG. 5. The Brillouin zone of thallium.

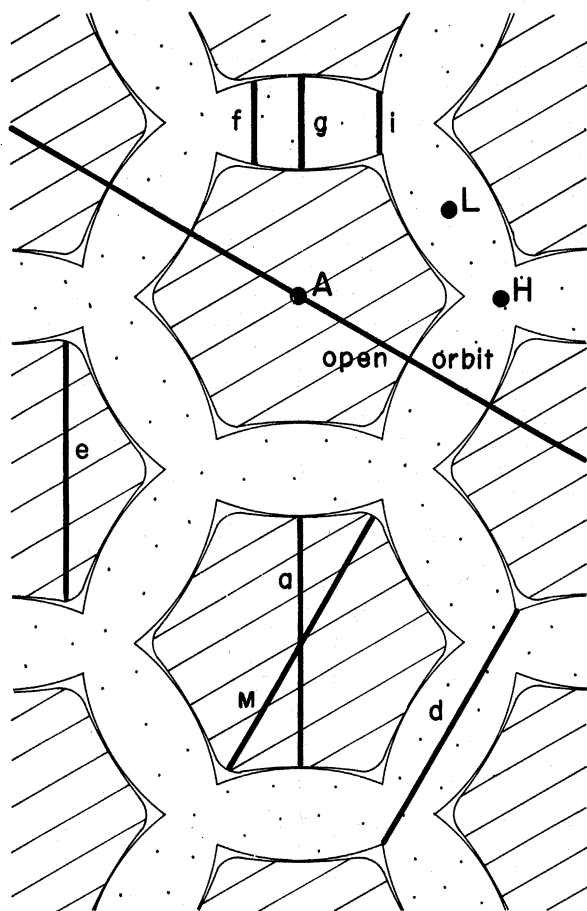


FIG. 6. A cross section of the thallium Fermi surface in the *AHL* planes. Orbits investigated in this research are indicated by a letter symbol. The notation corresponds to that used by Gage and Goodrich wherever possible.

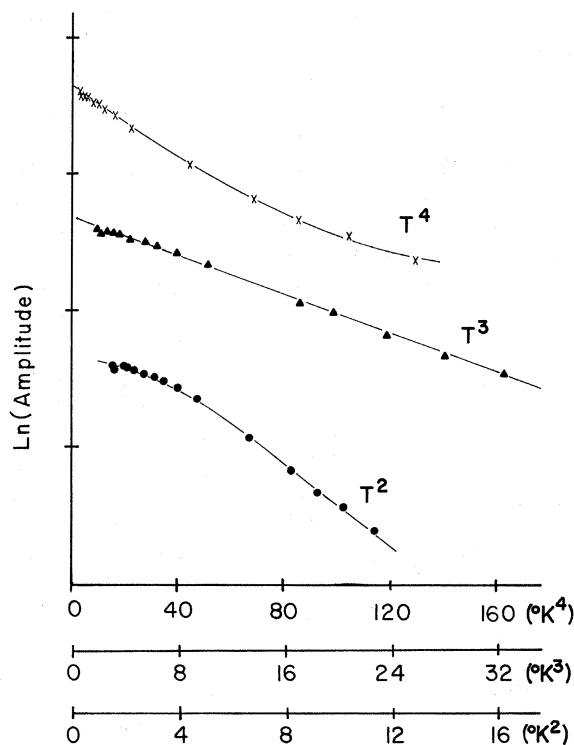


FIG. 7. A typical plot of the natural logarithm of the signal amplitude vs various powers of the temperature. The size of the marked data points are indicative of the uncertainty limits.

orbit.

The resonances which occur at magnetic fields greater than approximately 800 G indicate a temperature dependence for $1/\tau$ with exponent values greater than 3. A simple interpretation of the $n > 3$ exponent is that a single electron-phonon scattering event is no longer sufficient to render the electrons on the orbit ineffective. The higher exponent suggests the necessity of multiple scattering events similar to those observed in dc resistivity measurements at low temperatures. However the scattering effectiveness criterion for RFSE should differ from that for dc effects³ as discussed below.

A scattering-effectiveness criterion for the RFSE consistent with the data may be understood as follows. In order for an electron to contribute to the RFSE signal, it must pass through the skin-depth region of one sample surface and proceed along a trajectory which brings the electron into the skin-depth region of the opposite surface (Orbit A, Fig. 8). An electron initially on a resonant orbit will satisfy this criterion if unscattered. If an electron originally on a resonant orbit is scattered to a final trajectory which still passes through the skin-depth region of the second sample surface, the electron will still contribute to the

TABLE I. Summary of experimental results.

Direction of magnetic field	Orbit designation	Resonant field (G)	Caliper, k_D (10^8 cm^{-1})	Temperature dependence of $1/\tau$ ($1/\tau = \Gamma T^n$)	Slope of $\ln A$ vs T^n	$ C_0 $ (eV)
$[11\bar{2}0]$	<i>i</i>	199	0.49 ± 0.01	$n = 3.0 \pm 0.2$	0.116	4.40
$[11\bar{2}0]$	<i>f</i>	229	0.59 ± 0.01	$n = 3.0 \pm 0.2$	0.116	5.29
$[11\bar{2}0]$	<i>g</i>	284	0.70 ± 0.01	$n = 3.0 \pm 0.2$	0.097	4.82
$[11\bar{2}0]$	<i>g'</i>	433	1.06 ± 0.02	$n = 3.0 \pm 0.2$	0.101	3.28
$[11\bar{2}0]$	<i>a</i>	574	1.40 ± 0.02	$n = 3.0 \pm 0.2$	0.100	4.31
$[11\bar{2}0]$	<i>e</i>	612	1.51 ± 0.01	$n = 3.0 \pm 0.2$	0.069	4.65
$[11\bar{2}0]$	<i>f+a & i+a</i>	787	1.92 ± 0.04	$n = 4.0 \pm 0.2$	0.0230	...
$[11\bar{2}0]$	<i>i+e</i>	823	2.01 ± 0.03	$n = 5.0 \pm 0.2$	0.0078	...
$[11\bar{2}0]$	<i>C</i>	≈ 4000	High-field oscillations associated	$n = 3.0 \pm 0.2$ $n = 5.0 \pm 0.2$	0.063 0.0055	5.15 ...
$[11\bar{2}0]$	<i>D</i>	≈ 4000	with harmonics of open orbits	$n = 3.0 \pm 0.2$ $n = 5.0 \pm 0.2$	0.060 0.0064	5.03 ...
$[10\bar{1}0]$		284	0.70 ± 0.01	$n = 3.0 \pm 0.2$	0.086	2.00
$[10\bar{1}0]$	<i>M</i>	725	1.72 ± 0.02	$n = 3.0 \pm 0.2$	0.070	4.43
$[10\bar{1}0]$	<i>N</i>	764	1.81 ± 0.02	$n = 3.0 \pm 0.2$	0.156	6.96
$[10\bar{1}0]$	<i>d</i>	766	1.89 ± 0.02	$n = 3.0 \pm 0.2$	0.140	6.89
$[10\bar{1}0]$	<i>S</i>	≈ 1300	...	$n = 5.0 \pm 0.2$	0.0072	...

RFSE signal (Orbit B, Fig. 8). A phonon scattering process which renders an electron originally on a resonant orbit ineffective is shown as orbit C, Fig. 8, in which the final trajectory does not

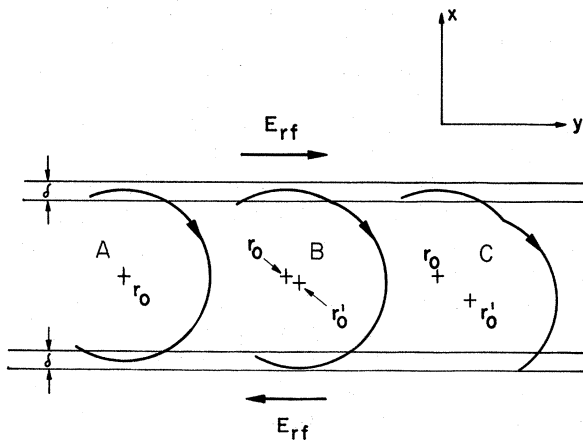


FIG. 8. A projection of the electron trajectory onto a plane perpendicular to the magnetic field for an unscattered resonant electron (Orbit A), an electron which is not removed from the resonant orbit by a single electron-phonon scattering event (Orbit B), and an electron which is removed from the resonant orbit by a single electron-phonon scattering event (Orbit C).

pass through the skin depth region of the second surface. The scattered electron thus cannot contribute to the RFSE signal. A model calculation based on this ineffectiveness criterion is presented below.

The equation of motion for an electron of wave vector \vec{k} and velocity \vec{v} in the presence of a magnetic field \vec{B} is

$$\hbar \frac{d\vec{k}}{dt} = \frac{-e}{c} \vec{v} \times \vec{B}. \quad (3)$$

For a constant magnetic field in the z direction, Eq. (3) can be integrated to find the trajectory coordinates in the xy plane:

$$x = \frac{c\hbar}{eB} k_y + x_0, \quad (4a)$$

$$y = \frac{-c\hbar}{eB} k_x + y_0, \quad (4b)$$

where the integration constant x_0 and y_0 are the (x, y) coordinates of geometrical center of the trajectory (Fig. 8). In an electron-phonon interaction the position of the electron (x, y, z) is instantaneously unchanged, but the wave vector (k_x, k_y, k_z) and the orbit center (x_0, y_0, z_0) change to (k'_x, k'_y, k'_z) and (x'_0, y'_0, z'_0) , respectively.

Using Eqs. (4a) and (4b) and the primed counterparts gives displacements of the trajectory center:

$$x'_0 - x_0 = \frac{-c\hbar}{eB} (k'_y - k_y), \quad (5a)$$

$$y'_0 - y_0 = \frac{c\hbar}{eB} (k'_x - k_x). \quad (5b)$$

The change in the electron wave vector due to a collision with a phonon of wave vector \vec{q} obeys the selection rule $\vec{k}' - \vec{k} = \vec{q}$. The effect of the interaction, then, is to displace the center of the electron trajectory by an amount

$$x'_0 - x_0 = \frac{-c\hbar}{eB} q_y, \quad (6a)$$

$$y'_0 - y_0 = \frac{c\hbar}{eB} q_x. \quad (6b)$$

The q_x component causes the trajectory center to move in the y direction, parallel to the sample surface. This will not move the trajectory extremes outside the skin depth. The q_y component is responsible for moving the trajectory extremes out of the skin depth.

The q_z component of the phonon wave vector can cause the electron to move to an orbit having a different radius. The resulting change in the trajectory radius in the x direction may move the trajectory extremes out of the skin depth. Assuming a free-electron model for the Fermi surface, the k -space orbit radius k_r is

$$k_r^2 = k^2 - k_z^2. \quad (7)$$

Combining Eq. (7) with the corresponding equation after the collision and conservation of energy yields

$$k_r'^2 - k_r^2 = -(q_x + k_z)q_x \pm 2mC_s q / \hbar. \quad (8)$$

For the case of central orbits, $k_r \gg k_z \gtrsim q_x$, one thus finds

$$k_r' \approx k_r - \frac{k_z q_x}{2k_r} - \frac{q_x^2}{2k_r} \pm \frac{mC_s q}{\hbar k_r}. \quad (9)$$

If x_m is the extremal value of the x coordinate of the orbit before collision, and x'_m is the extremal value after collision, then the criterion for an effective scattering event may be expressed as

$$|x'_m - x_m| \geq \frac{1}{2}\delta. \quad (10)$$

Using (6a) and (9) along with the ineffectiveness criterion yields

$$\left| q_y - \frac{q_x k_z}{2k_r} - \frac{q_x^2}{2k_r} \pm \frac{mC_s q}{\hbar k_r} \right| \geq \frac{eB\delta}{2c\hbar}. \quad (11)$$

For central orbits we may ignore all but the first term, and averaging the effect over the Debye sphere yields

$$q_{\min} = \frac{(3)^{1/2} eB\delta}{2c\hbar} \quad (12)$$

for the minimum value of q sufficient to render

an electron ineffective in a single electron-phonon scattering event. Note that q_{\min} is proportional to both the skin depth δ and the magnetic field B . As the resonance field increases, q_{\min} increases, resulting in a reduction in the number of phonons which can render an electron ineffective.

In order for the scattering model to be complete, one should demonstrate that the phonon distribution over the temperature range in which the data were obtained is consistent with the predicted value of q_{\min} . If the most probable value of q for a phonon at a temperature T is denoted by \bar{q} , then

$$\bar{q} = \frac{1.594 k_B T}{\hbar C_s} = 1.044 \times 10^8 T \text{ cm}^{-1} \quad (13)$$

for thallium. Setting the value of \bar{q} at 2.2°K (the midrange temperature for our experiments) equal to q_{\min} allows the transition value of the magnetic field to be determined. Using a value for the skin depth determined from experiment according to the relation $\delta = 0.15(\Delta B/B)d = 2.43 \times 10^{-4}$ cm, a transition field $B_t = 718$ G is predicted. The data show that the transition from T^3 to $T^{n>3}$ occurs between 600 and 800 G, in agreement with the prediction of the model.

The temperature dependence of the open-orbit resonance C or D shows a more complicated behavior. A plot of $\ln A$ versus T^n does not give a straight line over the range of temperatures investigated. An exponent of $n = 3$ appears to work well between 2 and 4.2°K, whereas $n = 5$ is required between 1.2 and 2.9°K. We are thus led to conclude that a transition occurs in which the dominant scattering mode changes from a single to a multiple-phonon process.

A semiquantitative explanation of this effect may be found in the following manner. The electrons contributing to the resonance travel along the AL open orbit which must pass through a point of degeneracy between the third and fourth bands. In theory, at 0°K the degeneracy region is a mathematical point, and the width of the open orbit band (Δk_x) in the direction parallel to the magnetic field is vanishingly small. However, at finite temperatures, the Fermi-Dirac distribution "smears" in a small range of energies about the Fermi energy. The "smearing" of the distribution function gives rise to an effective thermal broadening of the contact at the point of degeneracy. If a simple form for the Fermi surface is assumed near the point of degeneracy, the width of the open orbit at the degeneracy point becomes

$$\Delta k_x \approx 4(mk_B T / \hbar^2)^{1/2}. \quad (14)$$

Thus one might expect multiple-phonon scattering to be important at temperatures such that $\Delta k_x > \bar{q}$, whereas at temperatures for which $\Delta k_x < \bar{q}$, single-phonon processes should be the impor-

tant scattering mechanism. An order of magnitude T_0 may be found by equating the expressions for \bar{q} and Δk_z , which results in a transition temperature of $T_0 \approx 1.66$ °K. The data indicate that the transition occurs at a temperature between $T_0 = 2.0$ and $T_0 = 2.7$ °K, in approximate agreement with the theory.

IV. DISCUSSION AND CONCLUSIONS

The temperature dependence of the electron scattering time, τ , has been measured for several orbits in thallium. The results for closed orbits at low magnetic fields show a temperature dependence with an exponent $n = 3$ indicating that a single electron-phonon scattering event is sufficient to remove an electron from a resonance orbit. At values of the magnetic field above approximately 800 G, the temperature exponent assumes values greater than three, indicating the onset of multiple scattering events as the effective mechanism for removing the resonant electron from its orbit. Thus it would appear that the scattering time is dependent upon the magnetic field. Similar results have been reported by Phua and Peverley,¹¹ by Deaton,⁹ and by Cox and Gavenda⁸ in copper and by Witt and Peverley¹⁰ and by Tsoi and Gantmakher³ in potassium. In order to explain the results, a scattering-effectiveness criterion appropriate for a RFSE experiment was introduced. It was found that in order for a single phonon to scatter the electron from the resonant orbit, it was necessary for the magnitude of the phonon wave vector to have a minimum value proportional to the product $B\delta$. The most probable value of the phonon wave vector at a temperature T was calculated assuming a Debye model and was equated to q_{\min} . Thus a relation between the magnetic field and the temperature was found which was used to predict the value of the magnetic field at which the transition from single phonon to multiple phonon dominated processes is expected. A value of the temperature exponent of $n = 3$ was appropriate at low values of the magnetic field, and a transition to values of $n \geq 3$ at high values of the magnetic field was found in agreement with experiment. It is interesting to compare the results with those of other investigators. Phua and Peverley found a temperature dependence for $1/\tau_p$ with an exponent equal to 3 using geometric resonances in copper. Cox and Gavenda using the results of Deaton found $1/\tau_p$ to vary as the fifth power of the temperature in copper at high values

of the magnetic field also using a magnetoacoustic technique. A resolution of this apparent discrepancy may be found by adapting the effectiveness criterion for the RFSE to the magnetoacoustic effect. The sample thickness corresponds to the electron orbit diameter for a given geometric resonance peak. The diameter is given by $(p + \gamma)\lambda$ where p is the harmonic index integer, γ is a constant between zero and one, and λ is the wavelength of the ultrasonic wave. The skin depth would be replaced by a reasonable fraction, ϵ ($0 \leq \epsilon \leq 1$), of a wavelength of sound corresponding to the region of large $\vec{v} \cdot \vec{E}$ interaction between the electron and the ultrasonic wave. One then finds a relation between the magnetic field and the temperature for the transition from single to multiple phonon scattering, which can be written in terms of the harmonic index p as discussed by Phua and Peverley. Recalling that the results of Cox and Gavenda are obtained from high-magnetic-field data, one expects multiple scattering to be the dominant mechanism, whereas single-phonon scattering is dominant in the range of magnetic fields and temperatures investigated by Phua and Peverley. Willard¹² measured the temperature dependence of τ in thallium using an acoustic technique at magnetic fields up to 9.4 kG, and found a value of the temperature exponent equal to 3.6. On the basis of this work an exponent $n > 3$ is expected consistent with the observations of Willard; however, at very large magnetic fields a value larger than 3.6 would be expected. Bulk resistivity¹⁹ measurements in thallium give $n = 5$ as expected. The results of the open orbit study, although less conclusive due to the existence of only one open orbit, are consistent with the theory and with the results of Cox and Gavenda.

It is of further interest to note that the value of the deformation potential averaged over the orbit as observed for those orbits for which the geometric effects were normalized using the cyclotron mass and measured orbit caliper gave the same value of C_0 within experimental error. This suggests that the most appropriate measure of the scattering anisotropy might be C_0 rather than τ , since τ appears to depend upon not only the experimental technique used in the measurement and the value of the experimental parameters such as the magnetic field and the skin depth, but also on the orbit geometry factors such as k_p and m_c .

*Research supported in part by the Faculty Research Program at the University of Houston.

¹One of the authors (J.E.B.) wishes to acknowledge support by NSF Grant No. GZ-1335.

¹¹P. H. Haberland and C. A. Shiffman, Phys. Rev. Lett. **19**, 1337 (1967).

¹²V. F. Gantmakher and Yu. S. Leonov, Zh. Eksp. Teor. Fiz.

Pis'ma Red. **8**, 264 (1968) [JETP Lett. **8**, 162 (1968)].

³V. S. Tsoi and V. F. Gantmakher, Zh. Eksp. Teor. Fiz. **56**, 1232 (1969) [Sov. Phys.-JETP **29**, 663 (1969)].

⁴P. M. Snyder, J. Phys. F **1**, 363 (1971).

⁵V. F. Gantmakher and V. T. Dolgoplov, Zh. Eksp. Teor. Fiz. **60**, 2260 (1971) [Sov. Phys.-JETP **33**, 1215 (1971)].

⁶A. Myers, S. G. Porter, and R. S. Thompson, J. Phys. F

- 2, 24 (1972).
- ⁷V. P. Naberezhnykh and L. T. Tsymbal, *Zh. Eksp. Teor. Fiz. Pis'ma Red.* **5**, 319 (1967) [*JETP Lett.* **5**, 263 (1967)].
- ⁸W. R. Cox and J. D. Gavenda, *Phys. Rev. B* **3**, 3577 (1971).
- ⁹B. C. Deaton, *Phys. Rev.* **140**, A2051 (1965).
- ¹⁰T. J. Witt and J. R. Peverley, *Phys. Rev. B* **2**, 2974 (1970).
- ¹¹M. S. Phua and J. R. Peverley, *Phys. Rev. B* **3**, 3115 (1971).
- ¹²H. J. Willard, *Phys. Rev.* **175**, 367 (1968).
- ¹³G. G. Natale and I. Rudnick, *Phys. Rev.* **167**, 687 (1968).
- ¹⁴E. Y. Wang, R. J. Kolouch, and K. A. McCarthy, *Phys. Rev.* **175**, 723 (1968).
- ¹⁵E. Y. Wang and K. A. McCarthy, *Phys. Rev.* **183**, 653 (1969).
- ¹⁶P. Haussler and S. J. Welles, *Phys. Rev.* **152**, 675 (1966).
- ¹⁷D. C. Tsui and R. W. Stark, *Phys. Rev. Lett.* **19**, 1317 (1967).
- ¹⁸R. E. Hamburg, C. G. Grenier, and J. M. Reynolds, *Phys. Rev. Lett.* **23**, 236 (1969).
- ¹⁹N. V. Zavaritskii, *Zh. Eksp. Teor. Fiz.* **39**, 1571 (1960) [*Sov. Phys.-JETP* **12**, 1093 (1961)].
- ²⁰J. C. Garland and R. Bowers, *Phys. Kondens. Mater.* **9**, 36 (1969).
- ²¹R. E. Prange and T. W. Nee, *Phys. Rev.* **169**, 179 (1968).
- ²²T. W. Nee, J. F. Koch, and R. E. Prange, *Phys. Rev.* **174**, 758 (1968).
- ²³J. F. Koch, *Phys. Kondens. Mater.* **9**, 148 (1969).
- ²⁴J. F. Koch and J. D. Jensen, *Phys. Rev.* **184**, 643 (1969).
- ²⁵J. F. Koch and T. E. Murray, *Phys. Rev.* **186**, 722 (1969).
- ²⁶J. F. Koch and R. E. Doezema, *Phys. Rev. Lett.* **24**, 507 (1970).
- ²⁷K. E. Sibbald, A. L. Mears, and J. F. Koch, *Phys. Rev. Lett.* **27**, 14 (1971).
- ²⁸J. M. Ziman, *Electrons and Phonons* (Clarendon, Oxford, 1960).
- ²⁹V. F. Gantmakher, *Zh. Eksp. Teor. Fiz.* **43**, 345 (1962) [*Sov. Phys.-JETP* **16**, 247 (1963)].
- ³⁰C. Barrett, *Phys. Rev.* **110**, 1071 (1958).
- ³¹Shih-Yu Feng, *Rev. Sci. Instrum.* **40**, 963 (1969).
- ³²C. A. Gage and R. G. Goodrich, *Phys. Rev. B* **3**, 3214 (1971).
- ³³E. S. Takle and J. L. Stanford (unpublished).
- ³⁴R. C. Jones, R. G. Goodrich, and L. M. Falicov, *Phys. Rev.* **174**, 762 (1968).
- ³⁵J. R. Cleveland and J. L. Stanford, *Phys. Rev. B* **4**, 311 (1971).
- ³⁶I. P. Krylov and V. F. Gantmakher, *Zh. Eksp. Teor. Fiz.* **51**, 740 (1966) [*Sov. Phys.-JETP* **24**, 492 (1967)].

Elastic Constants and the Electrical Transition in Ti_2O_3 [†]

T. C. Chi and R. J. Sladek

Department of Physics, Purdue University, Lafayette, Indiana 47907

(Received 8 December 1972)

Measurements have been made of the transit times of pulses of longitudinal and transverse ultrasonic waves in single-crystal samples of Ti_2O_3 having appropriate orientations at various temperatures between 75 and 580 K. Sample-length-versus-temperature data were also obtained using a dilatometer. The elastic constants deduced from our measurements are found to exhibit anomalies connected with the gradual electrical transition which starts at about 400 K. Minima in C_{11} , C_{33} , and C_{12} and a maximum in C_{13} are accounted for semiquantitatively by means of a calculation of the contribution of Ti $3d$ electrons to the elastic constants using a deformation-potential approach and two $3d$ subbands whose separation decreases drastically with increasing temperature and becomes negative above the electrical transition. Electron-electron and/or electron-phonon interactions may be involved implicitly via the strong dependence of the energy gap on temperature. The temperature dependence of C_{44} is accounted for as a lattice effect, and C_{14} is so small that no attempt is made to interpret its temperature dependence. The room-temperature bulk modulus and Debye-temperature-versus-temperature results are reported.

I. INTRODUCTION

The purpose of this investigation¹ is to study elastic properties through a metal-nonmetal transition which is not accompanied by a change in crystal structure² nor in magnetic phase.³ Ti_2O_3 shows an interesting gradual electrical transition⁴ which extends from about 400 to 500 K. It has the rhombohedral α -corundum structure, and can be indexed in the hexagonal system.⁵ Although there is no change in crystal structure during the transition, the c axis expands and the a axis contracts.⁶

II. EXPERIMENTAL PROCEDURE

Single-crystal boules of Ti_2O_3 were obtained from the Purdue Central Crystal Growth Facility, where they were grown from the melt by the Czochralski method. Crystallographic directions in each boule were determined by x-ray diffraction. Samples of the order of 1 cm long were cut with a wire or diamond saw. Each was x-ray oriented, cemented into a brass lapping ring, and lapped on successively finer grinding powders on plates of glass and granite. Distilled water was used as a